Light scattering from a randomly occupied optical lattice. I. Born approximation

Wei Guo and Sudhakar Prasad
Department of Physics and Astronomy, The University of New Mexico, Albuquerque, New Mexico 87131
(Received 6 May 2002; revised manuscript received 22 January 2003; published 19 May 2003)

A theoretical study of the scattering of light from a randomly occupied optical lattice of resonant atoms is presented to reveal both the characteristics of the lattice and the properties of light scattered from the lattice. In the first-order Born approximation we discuss here, a number of interesting effects are established, including sideband Stokes scattering, a finite angular coherence of the scattered light, and spectral line narrowing. Specifically, the degree of angular coherence of the scattered light is calculated, and it is shown that such coherence is strongly influenced by the regularity and size of the underlying lattice structure. The previously observed phenomenon of the sideband spectral line narrowing is also explained in terms of the localization of atoms in the trapping potential wells. Important information about the lattice can thus be recovered by analyzing the scattered light in the Born approximation.

DOI: 10.1103/PhysRevE.67.056614 PACS number(s): 42.25.Dd, 42.25.Fx, 42.50.Ct

I. INTRODUCTION

Studies of light scattering have a modern history of over a hundred years since Rayleigh first successfully explained the blue sky and the associated light polarization puzzle. The single-scattering approximation that Rayleigh invoked is still popularly used because of its simplicity; it is not always sufficient, however, particularly when the medium is strongly scattering. Examples of strong scattering include the propagation of radiation through the atmospheres of stars and the scattering of sound in sea water [1].

The subject of radiative transfer was initially of interest mainly to the astronomical community. Active research in this area by the physics community was largely stimulated in the 1980s by the possibility of localizing light in a random, strongly scattering medium [2]. Weak localization [3–5], a phenomenon in which multiple scattering of radiation from a random medium generates an enhanced peak in the backscattering direction, was experimentally observed in 1985 by van Albada, Lagendijk, Wolf, and Maret [4,5]. Weak localization results from the fact that the fields multiply scattered by a given set of scatterers in one sequence and in the exact path-reversed sequence are in perfect phase, and therefore interfere constructively. Since these mutually reversed sequences of scattering can also form closed loops within the medium, the probability for the radiation to return to its starting point is greatly increased, and the diffusion constant is correspondingly reduced as discussed in Refs. [6,7]. Strong localization of light, characterized by a nearly complete lack of transmission of light through a strongly scattering medium, has also been observed recently in semiconductor powders [8].

An optical lattice is a periodic arrangement of atoms confined in place by laser beams. It is an important system because it provides a unique environment for performing precision spectroscopy, frequency standards, tests of fundamental physics, and more [9]. It is therefore desirable to characterize, both theoretically and experimentally, the dynamics of the trapped atoms inside the lattice. Light scattering, the topic of primary interest in the present paper, furnishes a convenient approach for this purpose. We will see that the important characteristics of the lattice, such as the structure of the optical potential, the lattice constant, sidebands, and the number of trapped atoms, can all be inferred from a study of the scattered light in the Born approximation.

When the atoms are trapped at the bottom of the trapping potential wells, a fully quantum-mechanical consideration reveals the presence of sidebands observed in the spectrum of the scattered light. However, since not all of the lattice sites are occupied and the knowledge of which sites are occupied by atoms and which sites are not can only be given in statistical terms, the scattered light too has a statistical character. In spite of the randomness of such a lattice based medium, a qualitative difference from a continuous random medium is that the underlying optical lattice possesses regularity. Here, we investigate how this regularity alters the character of light propagation in an otherwise random medium.

In the present paper, we discuss the scattering of light from an optical lattice in the first-order Born approximation, in which the second and higher orders of light scattering are regarded as being negligible. This is an accurate approximation when the atoms scatter only weakly and the occupation rate of the optical lattice is low, as is typically true in experiments with only about 10% of the sites occupied. For higher occupation rates or for strongly scattering atoms, multiple scattering of light can materially alter the character of the scattered light, as we show in paper II [10].

In problems involving randomly positioned but isotropic scatterers, since a scalar approximation to the electromagnetic field and the equations it obeys is generally accurate, the scattering problem is rarely considered beyond the scalar approximation [11–14]. We make the same approximation in our treatment of light scattering from an optical lattice of atoms. It is worth noting, however, that in certain situations of physical interest, it is no longer accurate to neglect the vector character of the radiation field. For example, when the medium is magnetoactive, then the presence of a magnetic field can excite the photonic Hall effect. This effect, theoretically predicted in Ref. [15] and experimentally demonstrated in Ref. [16], requires a full vector-field treatment. In the context of weak localization too, the application of a magnetic field breaks the time-reversal symmetry and causes the backscattering enhancement ratio, defined as the ratio of the enhanced scattering peak to its pedestal, to drop [17,18].

Our paper is organized as follows. In Sec. II, we formulate the problem and calculate the electric field at a point of observation in the far zone. The calculation of bilinear field averages taken over the statistical fluctuations of both the quantum motion and the randomness of the site occupation is presented in Sec. III. The total number of trapped atoms and other important parameters for an optical lattice can be related to the properties of the scattered light, as we show in Sec. IV. The angular coherence of the scattered light will also be discussed in that section. Then in Sec. V, we present an explanation of the phenomenon of linewidth narrowing. A few concluding remarks appear in Sec. VI.

II. THEORETICAL FORMULATION

In this paper, we study the scattering of a weak probe beam by an optical lattice of atoms in the first-order Born approximation. We treat the incident wave classically but the scattered field and the atoms quantum mechanically. We take the trapped atoms to be at a low enough temperature that they may be regarded as being essentially in the ground state of their trapping potential. Each atom performs a quantum-mechanical motion within its confining potential well. The motion of the center of mass of the atoms must therefore be properly treated. The quantized motion of atoms in both the two-dimensional [19,20] and three-dimensional [20] optical potential wells has been observed. The spectral sidebands arise just from this quantum motion. Since our analysis regards the field as an operator, it correctly describes important phenomena such as spontaneous decay.

Throughout the paper, we will assume for the sake of simplicity that the atoms are trapped in a simple cubic lattice. A detailed discussion of the crystallography of optical lattices can be found in Ref. [21]. In our calculations, we assume that the atoms have been trapped by some mechanism that need not be specified in advance. Since the movement of each atom is typically confined to a small region centered about the equilibrium point of its potential well, it is valid to approximate the potential well parabolically [22]. We make another useful simplification, one that is generally adequate for the resonant scattering treated here, that each atom has only two electronic energy states, namely, an excited state $|E\rangle$ and a ground state $|G\rangle$. This is a good approximation even when the atom has a degenerate ground state, i.e., when the magnetic quantum number for the ground state is nonzero. In that case, although each sublevel of the ground state will see a different confining potential, the transition rate from one such potential to another is rather low due to the Lamb-Dicke constraint [23], and one can assume that only one potential is present.

We treat our probe beam $\mathbf{E}_{inc}$ as a plane wave with a unit amplitude, wave vector $\mathbf{k}_0$, and polarization vector $\hat{\boldsymbol{\epsilon}}_0$

$$\mathbf{E}_{inc}=\hat{\boldsymbol{\epsilon}}_0 e^{i\mathbf{k}_0\cdot\mathbf{r}-i\omega t}. \tag{1}$$

Then, the Hamiltonian of the system, composed of the atom's internal energy, its external mechanical energy, and interaction with the probe field, takes the following form [24] in the weak field limit:

$$H=\hbar\omega_0 b^\dagger b+\frac{P^2}{2m}+\frac{\chi}{2}R^2-\mathbf{d}\cdot[\mathbf{E}_{inc}^{(+)}(\mathbf{R},t)b^\dagger+\mathbf{E}_{inc}^{(-)}(\mathbf{R},t)b], \tag{2}$$

where ω_0 is the atomic frequency, m is the mass of the atom, $\mathbf{P}$ and $\mathbf{R}$ are the momentum and position vector operators, respectively, and $\mathbf{d}$ is the dipole-moment vector matrix element for each atom. We treat each atom as an induced electric dipole with a physical extension that is much smaller than the wavelength of light. The variables $\mathbf{E}_{inc}^{(+)}$ and $\mathbf{E}_{inc}^{(-)}$ are the positive and negative frequency components of the incident field, respectively. The operators $b^\dagger=|E\rangle\langle G|$ and $b=|G\rangle\langle E|$ are the electronic raising and lowering operators.

By substituting the Hamiltonian into the Heisenberg equation of motion, we get a differential equation describing the time evolution of the lowering operator for the jth atom,

$$\dot{b}_j=(-i\omega_0-\gamma)b_j-\frac{\mathbf{d}\cdot\mathbf{E}_{inc,j}^{(+)}}{i\hbar}, \tag{3}$$

where γ, a damping constant, has been added phenomenologically to account for atomic spontaneous decay that arises from the interaction of the atom with its own field. A fluctuating vacuum-field contribution that enforces unitarity of interaction has been dropped from Eq. (3), as it contributes nothing to normally ordered operator expectation values. Also in Eq. (3), the incident field, with $\mathbf{E}_{inc,j}^{(+)}$ as its positive frequency component at the position of the jth atom, is assumed to be weak enough that the atom remains in its ground state with nearly unit probability.

If the intensity of the incident wave is low enough that the motion of the atoms is not perturbed much, then in the zeroth order approximation, we can assume that each atom moves harmonically with oscillation frequency $\bar{\omega}$, as it would in the absence of any incident wave,

$$\mathbf{r}_j(t)=\mathbf{r}_0\cos\bar{\omega}t+\frac{\mathbf{p}_0}{m\omega}\sin\bar{\omega}t. \tag{4}$$

Here, $\mathbf{r}_0$ represents the initial displacement and $\mathbf{p}_0$ the initial momentum of the atom j around the equilibrium point, $\mathbf{R}_j$, of its trapping potential. By evaluating the incident field (1) at the instantaneous location of the moving atom, substituting in Eq. (3), and noting that $\gamma\gg\bar{\omega}$, as is typically the case in experiments [25], we have the following approximate steady state solution for b_j:

$$b_j(t)\simeq-\frac{\mathbf{d}\cdot\hat{\boldsymbol{\epsilon}}_0}{i\hbar}e^{i\mathbf{k}_0\cdot\mathbf{R}_j-i\omega t}\frac{1}{\gamma+i(\omega_0-\omega)}\times e^{i(\mathbf{k}_0\cdot\mathbf{r}_0)\cos\bar{\omega}t+i(\mathbf{k}_0\cdot\mathbf{p}_0/m\bar{\omega})\sin\bar{\omega}t}. \tag{5}$$

Since the harmonic motion of the atom in its potential well leads to sidebands centered at frequencies that differ from the driving frequency by multiples of $\bar{\omega}$, the complex Lorentzian factor in Eq. (5) containing only a single driving frequency ω is approximate. More correctly, each sideband contribution in this equation, which can be made explicit by

expanding the second exponential in powers of $\exp(i\bar{\omega}t)$, must have its own Lorentzian factor, with ω replaced by its center frequency. Such a correction, however, is likely to be negligible when $\gamma \gg \bar{\omega}$ and when only the first few sidebands that are well within the atomic linewidth are significantly excited. We will assume throughout our work that these conditions are met.

When the atoms are excited by the incident light, they radiate as point dipoles, and the scattered field $\mathbf{E}_s(\mathbf{r},t)$ may be expressed as a superposition of such dipolar contributions. In calculating a quantum-mechanical expression for the mean scattered light intensity, we need the positive and negative frequency components $\mathbf{E}_s^{(\pm)}(\mathbf{r},t)$, of the scattered field operator. The Heisenberg equation of motion that $\mathbf{E}_s^{(+)}(\mathbf{r},t)$ obeys is the following:

$$\begin{aligned}\boldsymbol{\nabla}\times[\boldsymbol{\nabla}\times\mathbf{E}_s^{(+)}(\mathbf{r},t)]+\frac{1}{c^2}\frac{\partial^2\mathbf{E}_s^{(+)}(\mathbf{r},t)}{\partial t^2}&\\ \simeq -\frac{4\pi}{c^2}\mathbf{d}\sum_i \beta_i\ddot{b}_i(t)\,\delta(\mathbf{r}-\mathbf{R}_i-\mathbf{r}_i(t))&\\ \simeq \frac{4\pi\omega^2}{c^2}\mathbf{d}\sum_i \beta_i b_i(t)\,\delta(\mathbf{r}-\mathbf{R}_i-\mathbf{r}_i(t)),&\end{aligned} \tag{6}$$

where the summation has to be performed over all lattice sites and a binary number β_i has been introduced to specify whether the ith site is occupied ($\beta_i=1$) or unoccupied ($\beta_i=0$). In deriving Eq. (6), we have used the fact that since $\omega \gg \bar{\omega}$, the time oscillations of the electronic displacement of each atom are approximately those imposed by the external field in the absence of any atomic motion, so $\ddot{b}_i(t)\simeq -\omega^2 b_i(t)$.

When transformed to the frequency domain, Eq. (6) becomes

$$\begin{aligned}\boldsymbol{\nabla}\times[\boldsymbol{\nabla}\times\tilde{\mathbf{E}}_s^{(+)}(\mathbf{r},\tilde{\omega})]-\left(\frac{\tilde{\omega}}{c}\right)^2\tilde{\mathbf{E}}_s^{(+)}(\mathbf{r},\tilde{\omega})&\\ =\frac{4\pi\omega^2}{c^2\sqrt{2\pi}}\mathbf{d}\sum_i \beta_i\int b_i(t)\,\delta(\mathbf{r}-\mathbf{R}_i-\mathbf{r}_i(t))e^{i\tilde{\omega}t}dt,&\end{aligned} \tag{7}$$

where the one-dimensional Fourier transform has been defined as

$$\tilde{f}(k)=\frac{1}{\sqrt{2\pi}}\int f(x)e^{ikx}dx. \tag{8}$$

We can solve for $\tilde{\mathbf{E}}_s^{(+)}(\mathbf{r},\tilde{\omega})$ by using the dyadic Green's function [27] for the vector Helmholtz operator on the left-hand side of Eq. (7),

$$\begin{aligned}\mathbf{G}(\mathbf{r},\mathbf{r}',\tilde{\omega})&=\left(\mathbf{I}+\frac{1}{k_{\tilde{\omega}}^2}\boldsymbol{\nabla}\boldsymbol{\nabla}\right)\frac{e^{ik_{\tilde{\omega}}|\mathbf{r}-\mathbf{r}'|}}{4\pi|\mathbf{r}-\mathbf{r}'|}\\ &=\frac{1}{k_{\tilde{\omega}}^2}[(3-3ik_{\tilde{\omega}}|\mathbf{r}-\mathbf{r}'|-k_{\tilde{\omega}}^2|\mathbf{r}-\mathbf{r}'|^2)\hat{\rho}\hat{\rho}\\ &\quad-(1-ik_{\tilde{\omega}}|\mathbf{r}-\mathbf{r}'|-k_{\tilde{\omega}}^2|\mathbf{r}-\mathbf{r}'|^2)\mathbf{I}]\frac{e^{ik_{\tilde{\omega}}|\mathbf{r}-\mathbf{r}'|}}{4\pi|\mathbf{r}-\mathbf{r}'|^3},\end{aligned} \tag{9}$$

where $\hat{\rho}=(\mathbf{r}-\mathbf{r}')/|\mathbf{r}-\mathbf{r}'|$, $k_{\tilde{\omega}}=\tilde{\omega}/c$, and $\mathbf{I}$ is the unit dyadic. When the observation point $\mathbf{r}$ is far from the source point $\mathbf{r}'$, as always valid for a scattering problem, we may make a far-field approximation to $\mathbf{G}$,

$$\mathbf{G}(\mathbf{r},\mathbf{r}',\tilde{\omega})\simeq(\mathbf{I}-\hat{\mathbf{r}}\hat{\mathbf{r}})\frac{1}{4\pi r}e^{ik_{\tilde{\omega}}(r-\hat{\mathbf{r}}\cdot\mathbf{r}')}. \tag{10}$$

Use of the dyadic Green's function (10) enables us to solve Eq. (7) for the scattered field

$$\begin{aligned}\tilde{\mathbf{E}}_s^{(+)}(\mathbf{r},\tilde{\omega})&=\frac{4\pi\omega^2}{c^2\sqrt{2\pi}}\sum_i\int\mathbf{d}\cdot\mathbf{G}(\mathbf{r},\mathbf{r}_1,\tilde{\omega})d\mathbf{r}_1\\ &\quad\times\int\beta_i b_i(t)\,\delta(\mathbf{r}_1-\mathbf{R}_i-\mathbf{r}_i(t))e^{i\tilde{\omega}t}dt\\ &=\frac{\omega^2}{c^2\sqrt{2\pi}}(\mathbf{I}-\hat{\mathbf{r}}\hat{\mathbf{r}})\cdot\mathbf{d}\frac{e^{ik_{\tilde{\omega}}r}}{r}\sum_i\beta_i\\ &\quad\times\int b_i(t)e^{i\tilde{\omega}t-ik_{\tilde{\omega}}\hat{\mathbf{r}}\cdot[\mathbf{R}_i+\mathbf{r}_i(t)]}dt.\end{aligned} \tag{11}$$

Substituting expression (5) for b_i into Eq. (11) yields the following scattered field in the first Born approximation:

$$\begin{aligned}\tilde{\mathbf{E}}_s^{(+)}(\mathbf{r},\tilde{\omega})&=-\frac{\omega^2}{c^2}\frac{1}{\sqrt{2\pi}}\frac{\mathbf{d}\cdot\hat{\boldsymbol{\epsilon}}_0}{i\hbar}\frac{1}{\gamma+i(\omega_0-\omega)}\\ &\quad\times(\mathbf{I}-\hat{\mathbf{r}}\hat{\mathbf{r}})\cdot\mathbf{d}\frac{1}{r}e^{ik_{\tilde{\omega}}r}\sum_i\beta_i e^{i(\mathbf{k}_0-k_{\tilde{\omega}}\hat{\mathbf{r}})\cdot\mathbf{R}_i}\\ &\quad\times\int e^{i(\tilde{\omega}-\omega)t+i(\mathbf{k}_0-k_{\tilde{\omega}}\hat{\mathbf{r}})\cdot\mathbf{r}_i(t)}dt.\end{aligned} \tag{12}$$

The preceding equation may be expressed in terms of the lowering and raising operators, $a_i(t)$ and $a_i^\dagger(t)$, for the projection of the harmonic displacement vector (4) along the scattering vector

$$\mathbf{k}_1(\tilde{\omega})=\mathbf{k}_0-k_{\tilde{\omega}}\hat{\mathbf{r}}, \tag{13}$$

by writing

$$i(\mathbf{k}_0-k_{\tilde{\omega}}\hat{\mathbf{r}})\cdot\mathbf{r}_i(t)=i\mathbf{k}_1(\tilde{\omega})\cdot\mathbf{r}_i(t)=u_1(t)a_i^\dagger-u_1^*(t)a_i, \tag{14}$$

where $u_1(t)=ik_1\sqrt{(\hbar/2m\bar{\omega})}e^{i\bar{\omega}t}$. Upon substituting Eq. (14) into Eq. (12), we obtain the following expression for the scattered field operator:

$$\tilde{\mathbf{E}}_s^{(+)}(\mathbf{r},\tilde{\omega})=-\frac{\mathbf{d}\cdot\hat{\boldsymbol{\epsilon}}_0}{i\hbar}\frac{\omega^2}{c^2}\frac{1}{\sqrt{2\pi}}\frac{1}{\gamma+i(\omega_0-\omega)}\times(\mathbf{I}-\hat{\mathbf{r}}\hat{\mathbf{r}})\cdot\mathbf{d}\frac{1}{r}e^{ik_{\tilde{\omega}}r}\sum_i\beta_i e^{i\mathbf{k}_1\cdot\mathbf{R}_i}\times\int dt e^{a_i^\dagger u_1(t)-a_i u_1^*(t)}e^{i(\tilde{\omega}-\omega)t}. \quad (15)$$

Equation (15) will serve as the starting point for our calculation of bilinear scattered field averages.

III. CALCULATION OF BILINEAR FIELD AVERAGES

Under narrowband detection [28] the observed scattered light intensity is proportional to the quantum expectation value, $\langle\tilde{\mathbf{E}}_s^{(-)}(\mathbf{r},\tilde{\omega})\cdot\tilde{\mathbf{E}}_s^{(+)}(\mathbf{r},\tilde{\omega})\rangle$ in the initial state of the harmonic motion of the centers of mass of the trapped atoms. Let us assume initial state for each atom to be its ground state. Then, we may write with the help of Eq. (15)

$$\begin{aligned}&\langle\tilde{\mathbf{E}}_s^{(-)}(\mathbf{r},\tilde{\omega})\cdot\tilde{\mathbf{E}}_s^{(+)}(\mathbf{r},\tilde{\omega})\rangle\\&=\left(\frac{\mathbf{d}\cdot\hat{\boldsymbol{\epsilon}}_0}{\hbar}\right)^2\left(\frac{\omega}{c}\right)^4\frac{1}{2\pi}\frac{1}{\gamma^2+(\omega_0-\omega)^2}\frac{1}{r^2}|(\mathbf{I}-\hat{\mathbf{r}}\hat{\mathbf{r}})\cdot\mathbf{d}|^2\\&\times\sum_{i,j}\beta_i\beta_j e^{-i\mathbf{k}_1\cdot\mathbf{R}_i+i\mathbf{k}_1\cdot\mathbf{R}_j}\int dtdt' e^{-i(\tilde{\omega}-\omega)t+i(\tilde{\omega}-\omega)t'}\\&\times\langle e^{-u_1(t)a_i^\dagger+u_1^*(t)a_i}e^{a_j^\dagger u_1(t')-a_j u_1^*(t')}\rangle\\&\equiv B(\omega)\Bigg[\sum_i\beta_i\int dtdt' e^{-i(\tilde{\omega}-\omega)t+i(\tilde{\omega}-\omega)t'}\\&\times e^{-(k_1^2\hbar/2m\bar{\omega})+(k_1^2\hbar/2m\bar{\omega})e^{-i\bar{\omega}(t-t')}}\\&+\sum_{i\neq j}\beta_i\beta_j e^{-i\mathbf{k}_1\cdot(\mathbf{R}_i-\mathbf{R}_j)}\int dtdt' e^{-i(\tilde{\omega}-\omega)t+i(\tilde{\omega}-\omega)t'}\\&\times e^{-k_1^2\hbar/2m\bar{\omega}}\Bigg], \quad (16)\end{aligned}$$

where we have absorbed all coefficients in front of the first summation sign into $B(\omega)$. We have also used the fact that $\beta_i^2=\beta_i$, since $\beta_i=0$ or 1, in the first sum. Next we expand $\exp[(k_1^2\hbar/2m\bar{\omega})e^{-i\bar{\omega}(t-t')}]$ into a power series, and introduce two new parameters

$$T_1=\frac{1}{2}(t+t'), \quad (17)$$

$$T_2=t-t', \quad (18)$$

which permits us to rewrite Eq. (16) as

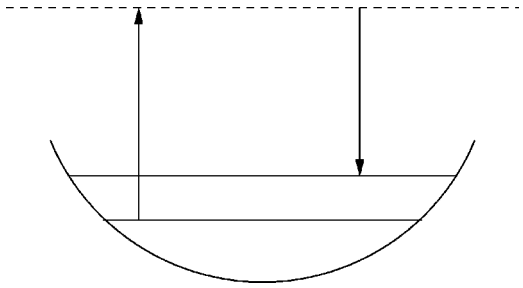

FIG. 1. The sideband generation, where the lower, upper, and dotted horizontal lines represent the states $|G\rangle\otimes|0\rangle$, $|G\rangle\otimes|n\rangle$, and $|E\rangle\otimes|m\rangle$, respectively.

$$\begin{aligned}&\langle\tilde{\mathbf{E}}_s^{(-)}(\mathbf{r},\tilde{\omega})\cdot\tilde{\mathbf{E}}_s^{(+)}(\mathbf{r},\tilde{\omega})\rangle\\&=e^{-(k_1^2\hbar/2m\bar{\omega})}\Bigg[\sum_i\beta_i\int dT_1dT_2e^{-i(\tilde{\omega}-\omega)T_2}\\&\times\sum_{n=1}^{\infty}\frac{1}{n!}\left(\frac{k_1^2\hbar}{2m\bar{\omega}}\right)^n e^{-in\bar{\omega}T_2}+\sum_{i\neq j}\beta_i\beta_j e^{-i\mathbf{k}_1\cdot(\mathbf{R}_i-\mathbf{R}_j)}\\&\times\int dT_1dT_2e^{-i(\tilde{\omega}-\omega)T_2}\Bigg]\\&=e^{-(k_1^2\hbar/2m\bar{\omega})}2\pi\\&\times\Bigg[\sum_i\beta_i\sum_{n=0}^{\infty}\frac{1}{n!}\left(\frac{k_1^2\hbar}{2m\bar{\omega}}\right)^n\delta(\tilde{\omega}-\omega+n\bar{\omega})\\&+\sum_{i\neq j}\beta_1\beta_j e^{-i\mathbf{k}_1\cdot(\mathbf{R}_i-\mathbf{R}_j)}\delta(\tilde{\omega}-\omega)\Bigg], \quad (19)\end{aligned}$$

where we have, for brevity, dropped $B(\omega)$ as well as an overall factor equal to the total observation time. The coefficient $\exp(-k_1^2\hbar/2m\bar{\omega})$ is the Debye-Waller factor that originates from the relative motion of the scatterers around the lattice sites [29].

Let there be altogether N atoms trapped in N_0 lattice sites. Usually N/N_0 is small, around 10% [30]. Then Eq. (19) takes the form

$$\begin{aligned}&\langle\tilde{\mathbf{E}}_s^{(-)}(\mathbf{r},\tilde{\omega})\cdot\tilde{\mathbf{E}}_s^{(+)}(\mathbf{r},\tilde{\omega})\rangle\\&\propto e^{-(k_1^2\hbar/2m\bar{\omega})}\Bigg[N\sum_{n=0}^{\infty}\frac{1}{n!}\left(\frac{k_1^2\hbar}{2m\bar{\omega}}\right)^n\delta(\tilde{\omega}-\omega+n\bar{\omega})\\&+\sum_{i\neq j}\beta_i\beta_j e^{-i\mathbf{k}_1\cdot(\mathbf{R}_i-\mathbf{R}_j)}\delta(\tilde{\omega}-\omega)\Bigg], \quad (20)\end{aligned}$$

where $\delta(\tilde{\omega}-\omega+n\bar{\omega})$ represents line emission at a sideband of frequency $(\omega-n\bar{\omega})$. The origin of sideband emission can be traced back to Raman scattering, as shown in Fig. 1. By absorbing a photon of frequency ω, an atom gets electronically excited from the ground state $|G\rangle\otimes|0\rangle$ to a higher energy level $|E\rangle\otimes|m\rangle$, then jumps back to a vibrationally

excited state $|G\rangle\otimes|n\rangle$ in the electronic ground state, giving up a photon with frequency $(\omega-n\bar{\omega})$, $n>0$. Here, $|0\rangle$ represents the ground state of harmonic oscillation of the atom and $|n\rangle$ an excited state. In experiments anti-Stokes sidebands at frequencies $(\omega+n\bar{\omega})$ are also found [32], because in reality not all atoms are in the ground state of harmonic oscillation.

Equation (20) reveals two distinct kinds of scattering. The first is elastic scattering, represented by the $n=0$ term of the first sum and by the entire second sum. The second sum gives the usual Bragg scattering, which is weak for small occupation fractions. The second kind of scattering is inelastic scattering, represented by the $n\neq 0$ terms in the first sum. When an atom is raised from the ground state to an excited state by the absorption of a photon from the incoming wave, it can return to its original state by emitting a coherent photon of the same frequency as the incident wave. Alternatively, the excited atom can relax back to an excited state of harmonic motion in the electronic ground state, in which case the scattered photon has not only a different frequency but also has no definite phase relation with the incident wave. This is why radiation scattered at the central frequency is enhanced by a coherent interference of contributions from different atoms, while there is no such interference at any of the sidebands, as clearly seen in Eq. (20).

Equation (20) represents the expectation value of the light intensity at frequency $\tilde{\omega}$ from a given realization of the site occupation. We must average Eq. (20) over $\beta_i\beta_j$ to arrive at the average intensity that one would observe in any practical experiment. It is readily found that for $i\neq j$

$$\langle\beta_i\beta_j\rangle=\langle\beta_i\rangle\langle\beta_j\rangle=(N/N_0)^2\equiv\beta_0^2,$$

assuming that each site is equally likely to be occupied. Using a single pair of triangular brackets to denote both a quantum-mechanical expectation value and an average over the fluctuations of the site occupation, we find the following mean scattered light intensity:

$$\langle\tilde{\mathbf{E}}_s^{(-)}(\mathbf{r},\tilde{\omega})\cdot\tilde{\mathbf{E}}_s^{(+)}(\mathbf{r},\tilde{\omega})\rangle\propto e^{-k_1^2\hbar/2m\bar{\omega}}\left[N\sum_{n=0}^{\infty}\frac{1}{n!}\left(\frac{k_1^2\hbar}{2m\bar{\omega}}\right)^n\times\delta(\tilde{\omega}-\omega+n\bar{\omega})+\sum_{i\neq j}(N/N_0)^2\times e^{-i\mathbf{k}_1\cdot(\mathbf{R}_i-\mathbf{R}_j)}\delta(\tilde{\omega}-\omega)\right].\qquad(21)$$

Note that in a statistical sense, we have a uniform lattice on an average, one that should produce Bragg scattering. The second sum in the above square brackets is just the mathematical expression for that scattering.

The nth sideband contribution to the mean scattered intensity is weighted by a factor of $(\hbar k_1^2/2m\bar{\omega})^n$ in Eq. (21). This means the part of the energy radiated in the sidebands is significantly controlled by the potential well. The stiffer the potential, i.e., the larger $\bar{\omega}$, the fewer the sidebands that are significantly excited [33]. Since $\hbar k_1^2/2m\bar{\omega}$ is proportional to the squared ratio of the oscillation amplitude of the atoms to the optical wavelength, the number of scattered sidebands that are observed is a strong indicator of how well the atoms are localized, on the scale of an optical wavelength, in the optical potential wells. The more tightly the atoms are confined, the smaller that number [22]. This is often referred to as the Dicke effect [34,35].

IV. NUMBER OF TRAPPED ATOMS AND ANGULAR COHERENCE OF SCATTERED LIGHT

Several important conclusions can be drawn from the results of the preceding section. First of all, the difference between two successive sideband frequencies tells us the structure of the optical potential at each lattice site through $\bar{\omega}=\sqrt{\chi/m}$. Second, from the Bragg scattering term in Eq. (21), the lattice constant can be measured by recording the angular variation of the intensity at the central frequency. The first term of Eq. (21) provides a uniform background in the angular pattern of the scattered light intensity, and can be easily subtracted out. We now consider two other useful results that require a somewhat more detailed discussion.

A. Number of trapped atoms

The number of trapped atoms can be inferred experimentally by using the Bragg diffraction technique [36]. Here, we present another simple way to obtain this information. In the exact forward scattering direction of the incident wave, we measure the intensity of the scattered light at the central frequency I_{elas} and the intensity at the first sideband I_{inela}. For the central frequency $\tilde{\omega}=\omega$, $k_1=0$ for forward scattering, and so from Eq. (21),

$$I_{elas}\propto N^2.$$

For the first sideband, on the other hand, $k_1=\tilde{\omega}/c$ for forward scattering, and so again from Eq. (21),

$$I_{inela}\propto N\frac{\bar{\omega}\hbar}{2mc^2}e^{-\bar{\omega}\hbar/2mc^2}.$$

By taking the ratio of the two, we have

$$N=\frac{I_{elas}}{I_{inela}}\frac{\bar{\omega}\hbar}{2mc^2}e^{-\bar{\omega}\hbar/2mc^2},$$

where $\omega\gg\bar{\omega}$ and $N\gg 1$ are assumed. Thus, by measuring I_{elas}, I_{inela}, and $\bar{\omega}$, one can deduce the number of trapped atoms.

B. Angular coherence of scattered light

We may calculate the degree of angular coherence of the scattered light by considering the field correlation along two observation directions, specified by unit vectors $\hat{\mathbf{r}}$ and $\hat{\mathbf{r}}'$. By taking the scalar product of $\tilde{\mathbf{E}}_s^{(+)}(\hat{\mathbf{r}},\tilde{\omega})$ given by Eq. (15)

with its Hermitian adjoint evaluated along the $\hat{\mathbf{r}}'$ direction, and then taking the expectation value of the resulting bilinear operator product in the initial ground state of the center-of-mass motion of atoms, we obtain

$$\langle \tilde{\mathbf{E}}_s^{(-)}(\hat{\mathbf{r}},\tilde{\omega})\cdot\tilde{\mathbf{E}}_s^{(+)}(\hat{\mathbf{r}}',\tilde{\omega})\rangle \sim \sum_{i,j}\beta_i\beta_j e^{-i\mathbf{k}_1\cdot\mathbf{R}_i+i\mathbf{k}_1'\cdot\mathbf{R}_j}\int\int dtdt' e^{-i(\tilde{\omega}-\omega)t+i(\tilde{\omega}-\omega)t'} \times\langle e^{-u_1(t)a_i^\dagger+u_1^*(t)a_i e^{a_j^\dagger u_1'(t')-a_j u_1'^*(t')}}\rangle, \tag{22}$$

where we have suppressed for brevity an overall coefficient on the right-hand side. The preceding average has two contributions. One is from the fields that originate from the same atoms, corresponding to the $i=j$ terms. The other is from the interference of the fields radiated by different atoms, corresponding to the $i\neq j$ terms. By recognizing that the operator whose expectation value is needed in Eq. (22) may be expressed in terms of the coherent state displacement operator $D(\alpha)$ [37], we can evaluate that expectation value rather simply. For $i=j$, one has

$$\begin{aligned}\langle e^{-u_1(t)a_i^\dagger+u_1^*(t)a_i e^{a_j^\dagger u_1'(t')-a_j u_1'^*(t')}}\rangle &\equiv\langle D_i[-u_1(t)]D_i[u_1'(t')]\rangle \\ &= e^{[(k_1k_1'\hbar/2m\bar{\omega})e^{i\bar{\omega}(t'-t)}-\hbar(k_1^2+k_1'^2)/4m\bar{\omega}]},\end{aligned} \tag{23}$$

while, when $i\neq j$

$$\begin{aligned}\langle e^{-u_1(t)a_i^\dagger+u_1^*(t)a_i e^{a_j^\dagger u_1'(t')-a_j u_1'^*(t')}}\rangle &=\langle e^{-u_1(t)a_i^\dagger+u_1^*(t)a_i}\rangle\langle e^{a_j^\dagger u_1'(t')-a_j u_1'^*(t')}\rangle \\ &= e^{-\hbar(k_1^2+k_1'^2)/4m\bar{\omega}}.\end{aligned} \tag{24}$$

With these results, expression (22) takes the form

$$\begin{aligned}\langle \tilde{\mathbf{E}}_s^{(-)}(\hat{\mathbf{r}},\tilde{\omega})\cdot\tilde{\mathbf{E}}_s^{(+)}(\hat{\mathbf{r}}',\tilde{\omega})\rangle \sim\Bigg[&\sum_i\beta_i e^{i(\mathbf{k}_1'-\mathbf{k}_1)\cdot\mathbf{R}_i}\int dtdt' e^{i(\tilde{\omega}-\omega)(t'-t)} \times e^{-\hbar(k_1^2+k_1'^2)/4m\bar{\omega}+(k_1k_1'\hbar/2m\bar{\omega})e^{i\bar{\omega}(t'-t)}} \\ &+\sum_{i\neq j}\beta_i\beta_j e^{-i\mathbf{k}_1\cdot\mathbf{R}_i+i\mathbf{k}_j'\cdot\mathbf{R}_j}\int dtdt' e^{i(\tilde{\omega}-\omega)(t'-t)} \times e^{-\hbar(k_1^2+k_1'^2)/4m\bar{\omega}}\Bigg].\end{aligned} \tag{25}$$

We now expand $\exp[(k_1k_1'\hbar/2m\bar{\omega})e^{i\tilde{\omega}(t'-t)}]$, as before, into a power series, and introduce the sum and difference times $T_1=(t+t')/2$ and $T_2=(t-t')$. An integration over T_2 then reveals the presence of sidebands in the correlation function (25),

$$\begin{aligned}\langle \tilde{\mathbf{E}}_s^{(-)}(\hat{\mathbf{r}},\tilde{\omega})\cdot\tilde{\mathbf{E}}_s^{(+)}(\hat{\mathbf{r}}',\tilde{\omega})\rangle \sim e^{-(\hbar/4m\bar{\omega})(k_1^2+k_1'^2)}\Bigg[&\sum_i\beta_i e^{i(\mathbf{k}_1'-\mathbf{k}_1)\cdot\mathbf{R}_i}\sum_n\frac{1}{n!} \times\left(k_1k_1'\frac{\hbar}{2m\bar{\omega}}\right)^n\delta(\tilde{\omega}-\omega+n\bar{\omega}) \\ &+\sum_{i\neq j}\beta_i\beta_j e^{-i\mathbf{k}_1\cdot\mathbf{R}_i+i\mathbf{k}_j'\cdot\mathbf{R}_j}\delta(\tilde{\omega}-\omega)\Bigg].\end{aligned} \tag{26}$$

When averaged over the occupation of lattice sites, the mean correlation function (26) becomes

$$\begin{aligned}\langle \tilde{\mathbf{E}}_s^{(-)}(\hat{\mathbf{r}},\tilde{\omega})\cdot\tilde{\mathbf{E}}_s^{(+)}(\hat{\mathbf{r}}',\tilde{\omega})\rangle \sim e^{-(\hbar/4m\bar{\omega})(k_1^2+k_1'^2)}\Bigg[&\beta_0\sum_n\frac{1}{n!}(k_1k_1'\hbar/2m\bar{\omega})^n \times\delta(\tilde{\omega}-\omega+n\bar{\omega})\sum_i e^{i(\mathbf{k}_1'-\mathbf{k}_1)\cdot\mathbf{R}_i} \\ &+\beta_0^2\sum_{i\neq j}e^{-i\mathbf{k}_1\cdot\mathbf{R}_i+i\mathbf{k}_1'\cdot\mathbf{R}_j}\delta(\tilde{\omega}-\omega)\Bigg].\end{aligned} \tag{27}$$

By adding to and subtracting from the double sum in Eq. (27) terms with $i=j$, we may reexpress it in terms of unrestricted sums over all lattice sites as

$$\begin{aligned}\langle \tilde{\mathbf{E}}_s^{(-)}(\hat{\mathbf{r}},\tilde{\omega})\cdot\tilde{\mathbf{E}}_s^{(+)}(\hat{\mathbf{r}}',\tilde{\omega})\rangle \sim e^{-(\hbar/4m\bar{\omega})(k_1^2+k_1'^2)}\Bigg[&\beta_0\sum_n\frac{1}{n!}(k_1k_1'\hbar/2m\bar{\omega})^n \times\delta(\tilde{\omega}-\omega+n\bar{\omega})\sum_i e^{i(\mathbf{k}_1'-\mathbf{k}_1)\cdot\mathbf{R}_i}+\beta_0^2\left(\sum_i e^{-i\mathbf{k}_1\cdot\mathbf{R}_i}\right) \\ &\times\left(\sum_j e^{i\mathbf{k}_1'\cdot\mathbf{R}_j}\right)\delta(\omega-\tilde{\omega})-\beta_0^2\sum_i e^{i(\mathbf{k}_1'-\mathbf{k}_1)\cdot\mathbf{R}_i} \times\delta(\tilde{\omega}-\omega)\Bigg].\end{aligned} \tag{28}$$

These lattice sums are simple geometric-series sums and are thus easily evaluated. If we choose the origin of the coordinate system to be at the center of the lattice, and there are N_x+1, N_y+1, and N_z+1 sites along the three sides [38], then we have

$$\sum_i e^{i\mathbf{k}\cdot\mathbf{R}_i}=\Theta(\mathbf{k}), \tag{29}$$

where $\Theta(\mathbf{k})$ is the three-dimensional grating function defined as

$$\Theta(\mathbf{k})=\frac{\sin[k_x a(N_x+1)/2]}{\sin(k_x a/2)}\,\frac{\sin[k_y a(N_y+1)/2]}{\sin(k_y a/2)}\times\frac{\sin[k_z a(N_z+1)/2]}{\sin(k_z a/2)}.$$

Using this sum formula, we may write down for the correlation function

$$\langle\tilde{\mathbf{E}}_s^{(-)}(\hat{\mathbf{r}},\tilde{\omega})\cdot\tilde{\mathbf{E}}_s^{(+)}(\hat{\mathbf{r}}',\tilde{\omega})\rangle \sim e^{-(\hbar/4m\bar{\omega})(k_1^2+k_1'^2)}\left\{\beta_0\sum_n\frac{1}{n!}\left(k_1k_1'\frac{\hbar}{2m\bar{\omega}}\right)^n \times\delta(\tilde{\omega}-\omega+n\bar{\omega})\Theta(\mathbf{k}_1'-\mathbf{k}_1)+\beta_0^2\delta(\tilde{\omega}-\omega) \times[\Theta(\mathbf{k}_1')\Theta(-\mathbf{k}_1)-\Theta(\mathbf{k}_1'-\mathbf{k}_1)]\right\}. \tag{30}$$

Expressions for the mean intensities along the two observation directions now follow from this result when the two directions $\hat{\mathbf{r}}$ and $\hat{\mathbf{r}}'$ are set equal in Eq. (30). The mean intensity along $\hat{\mathbf{r}}$ takes the form

$$\langle\tilde{\mathbf{E}}_s^{(-)}(\hat{\mathbf{r}},\tilde{\omega})\cdot\tilde{\mathbf{E}}_s^{(+)}(\hat{\mathbf{r}},\tilde{\omega})\rangle \sim e^{-(\hbar/2m\bar{\omega})k_1^2}\left[\beta_0\sum_n\frac{1}{n!}(k_1^2\hbar/2m\bar{\omega})^n\delta(\tilde{\omega}-\omega+n\bar{\omega})N_0 +\beta_0^2\Theta^2(\mathbf{k}_1)\delta(\tilde{\omega}-\omega)-\beta_0^2\delta(\tilde{\omega}-\omega)N_0\right], \tag{31}$$

where we have used the result that $\Theta(\mathbf{0})=(N_x+1)(N_y+1)(N_z+1)=N_0$, the total number of lattice sites. The mean intensity along $\hat{\mathbf{r}}'$ is obtained by replacing $\hat{\mathbf{r}}$ in Eq. (31) by $\hat{\mathbf{r}}'$.

With the help of these expressions, we may write down an explicit result for the degree of angular coherence γ_{coh} defined as the ratio

$$\gamma_{coh}(\hat{\mathbf{r}},\hat{\mathbf{r}}')=\frac{|\langle\tilde{\mathbf{E}}_s^{(-)}(\hat{\mathbf{r}},\tilde{\omega})\cdot\tilde{\mathbf{E}}_s^{(+)}(\hat{\mathbf{r}}',\tilde{\omega})\rangle|}{\sqrt{\langle\tilde{\mathbf{E}}_s^{(-)}(\hat{\mathbf{r}},\tilde{\omega})\cdot\tilde{\mathbf{E}}_s^{(+)}(\hat{\mathbf{r}},\tilde{\omega})\rangle\langle\tilde{\mathbf{E}}_s^{(-)}(\hat{\mathbf{r}}',\tilde{\omega})\cdot\tilde{\mathbf{E}}_s^{(+)}(\hat{\mathbf{r}}',\tilde{\omega})\rangle}}. \tag{32}$$

If one only looks at the central frequency, i.e., the incident frequency ω, then the explicit formula for γ_{coh} assumes the form

$$\gamma_{coh}(\omega)=\left|\frac{[(\mathbf{I}-\hat{\mathbf{r}}\hat{\mathbf{r}})\cdot\mathbf{d}]\cdot[(\mathbf{I}-\hat{\mathbf{r}}'\hat{\mathbf{r}}')\cdot\mathbf{d}]}{|(\mathbf{I}-\hat{\mathbf{r}}\hat{\mathbf{r}})\cdot\mathbf{d}||(\mathbf{I}-\hat{\mathbf{r}}'\hat{\mathbf{r}}')\cdot\mathbf{d}|}\,\frac{(1-\beta_0)\Theta(\mathbf{k}_1'-\mathbf{k}_1)+\beta_0\Theta(\mathbf{k}_1')\Theta(-\mathbf{k}_1)}{\sqrt{(1-\beta_0)N_0+\beta_0\Theta^2(\mathbf{k}_1)}\sqrt{(1-\beta_0)N_0+\beta_0\Theta^2(\mathbf{k}_1')}}\right|. \tag{33}$$

The degree of angular coherence takes a somewhat simpler form for the first sideband frequency $\omega-\bar{\omega}$,

$$\gamma_{coh}(\omega-\bar{\omega})=\left|\frac{[(\mathbf{I}-\hat{\mathbf{r}}\hat{\mathbf{r}})\cdot\mathbf{d}]\cdot[(\mathbf{I}-\hat{\mathbf{r}}'\hat{\mathbf{r}}')\cdot\mathbf{d}]\Theta(\mathbf{k}_1'-\mathbf{k}_1)}{|(\mathbf{I}-\hat{\mathbf{r}}\hat{\mathbf{r}})\cdot\mathbf{d}||(\mathbf{I}-\hat{\mathbf{r}}'\hat{\mathbf{r}}')\cdot\mathbf{d}|N_0}\right|. \tag{34}$$

The angular coherence function exhibits a dependence on the number of lattice sites N_x,N_y,N_z even in the limit that they go to ∞, but that dependence is principally through the multiple occurrences of the grating function Θ in Eqs. (33) and (34). According to its definition, the grating function (29) is a product of three one-dimensional grating functions depending separately on N_x,k_x, N_y,k_y, and N_z,k_z. The first of such functions,

$$\frac{\sin[k_x a(N_x+1)/2]}{\sin(k_x a/2)},$$

has principal maxima at $k_x a=2p\pi$ and secondary maxima at $k_x a(N_x+1)=2q\pi$, where p is any integer, while q is any integer not equal to a multiple of (N_x+1). Both kinds of maxima have an angular width of the order of $\lambda/(N_x a)$ that becomes infinitely small in the limit $N_x\to\infty$. The other two functions of which Θ is composed exhibit similar dependences. In spite of these vanishing angular widths, however, the grating function itself does not vanish in the limit $N_x,N_y,N_z\to\infty$. The locations of the principal maxima of the grating function $\Theta(\mathbf{k}_1'-\mathbf{k}_1)$ correspond to the Bragg scattering condition, for which both the denominator and the numerator in Eqs. (33) and (34) approach infinity at the same rate, leading to a finite γ_{coh}.

We shall now display some of our results in graphical form. We choose the incident wave vector and the first scattering direction to be along the z axis: $\mathbf{k}_0=k_0\hat{\mathbf{z}}$, $\hat{\mathbf{r}}=\hat{\mathbf{z}}$. The second scattering direction is then selected to lie in the xz plane at angle θ with the first, $\hat{\mathbf{r}}'=\sin\theta\hat{\mathbf{x}}+\cos\theta\hat{\mathbf{z}}$. Therefore, from Eq. (13), $\mathbf{k}_1=\mathbf{0}$, $\mathbf{k}_1'=k_0(-\sin\theta,0,1-\cos\theta)$. Since the orientation of the dipole moment matrix element $\mathbf{d}$ of each scatterer is, in general, not fixed, in any experiment involving many scatterers, we must regard $\mathbf{d}$ as randomly oriented in a statistically isotropic manner in space and thus average all expectation values of interest over all possible orientations of $\mathbf{d}$. We do this averaging numerically.

We see in Fig. 2, where $a/\lambda=1.7$, it is only in the forward direction ($\theta=0$) that there is perfect coherence, but there are secondary peaks distributed between $\theta=0$ and $\theta=\pi$. The

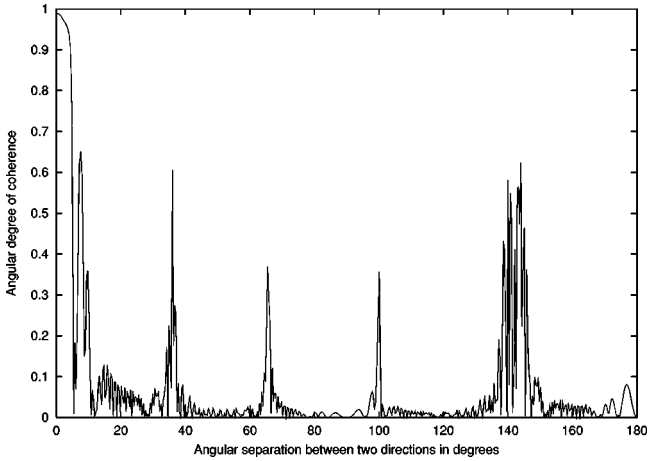

FIG. 2. Degree of angular coherence at the central frequency with $a/\lambda = 1.70$ and 101 sites on each side of the lattice.

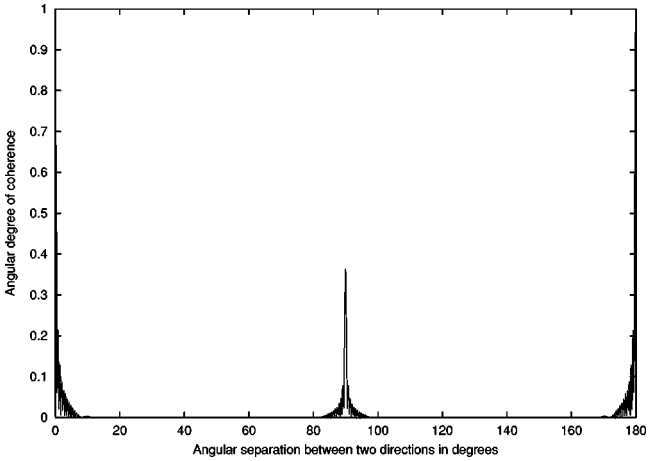

FIG. 4. Degree of angular coherence at the first sideband with $a/\lambda = 1.0$ and 101 sites on each side of the lattice.

forward peak rather trivially meets the Bragg scattering condition $\mathbf{k}_0 - \mathbf{k}_s = \mathbf{G}$, where $\mathbf{G}$ is a reciprocal lattice vector. The secondary peaks result, by contrast, from only an imperfect satisfaction of that condition in the x-z plane, which implies a correspondingly imperfect coherence between the forward and obliquely scattered beams. In Fig. 3, where $a/\lambda = 1$, perfect coherence is obtained in both the forward and backward directions. The backward coherence always exists whenever a/λ is an integral number, under this condition the backward scattered waves are entirely in phase with the forward waves. The Bragg condition is satisfied for one more direction in the x-z plane, that is along the $\hat{\mathbf{x}}$ axis ($\theta = \pi/2$). This shows up as a secondary peak at $\theta = \pi/2$. The fact that $|\gamma_{coh}|$ is strictly less than 1 has to do with the scattering-angle dependent angular averaging of the dipole-moment orientations in Eq. (33), even though the purely phase dependent factor, which depends on the Θ's in that equation, is exactly 1 for this case as for $\theta = 0$ and π.

We plot the degree of angular coherence at the first sideband, $\gamma_{coh}(\omega - \overline{\omega})$, in Figs. 4 and 5. Unlike the case of $\gamma_{coh}(\omega)$, there are no atom-atom interference terms for $\gamma_{coh}(\omega - \overline{\omega})$. Since $\overline{\omega}/c$ is a very small number, however, the incident and scattered waves have practically the same frequency.

One significant difference between the coherence patterns at ω and $\omega - \overline{\omega}$, apart from the obvious Bragg enhancement for the former, is that in the forward scattering the degree of angular coherence at $\omega - \overline{\omega}$ decays rapidly with the angle between the observation directions. This behavior of γ_{coh} can be understood based on the Van Cittert-Zernike theorem [39], according to which light emitted by a collection of spatially distributed incoherent radiators, such as those we have here at all of the sidebands $\omega - n\overline{\omega}, n \neq 0$, will acquire partial spatial coherence on propagation in a manner described by a Fourier transform relation. The angular width of this coherence around the forward direction is of the order of $\lambda/N_x a$, which is about 0.01 rad in Fig. 4 and 0.006 rad in Fig. 5. Since the total field radiated by a discrete but periodic array of atoms, even when emitting with random phases, is coherent along any two directions that obey the Bragg condition, a similar structure is obtained around each Bragg direction. This may be seen as the additional structure in the

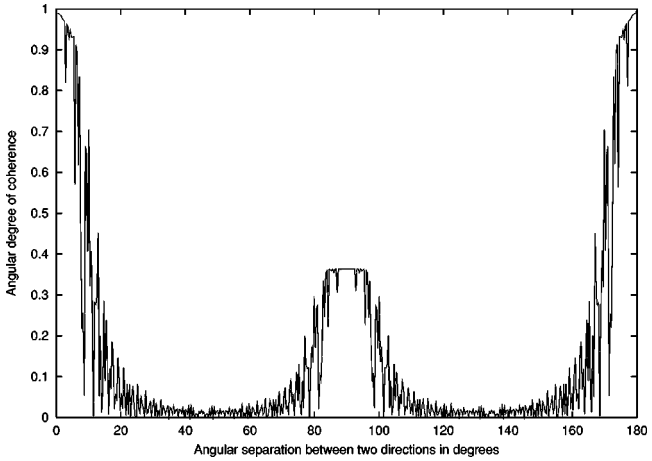

FIG. 3. Degree of angular coherence at the central frequency with $a/\lambda = 1.0$ and 101 sites on each side of the lattice.

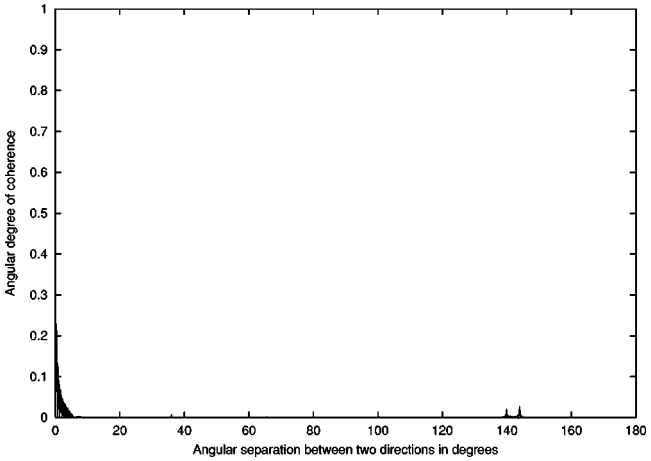

FIG. 5. Degree of angular coherence at the first sideband with $a/\lambda = 1.70$ and 101 sites on each side of the lattice.

angular coherence function around $\Delta\theta=\pi/2$ and π in Fig. 4.

V. NARROWING OF SIDEBAND SPECTRAL LINES

It was found in Ref. [33] that the spectral widths of the sidebands are actually narrower than that expected, based on a free-atom theory. This line narrowing can be traced to the Lamb-Dicke effect that relates to the spatial localization of the atoms in optical traps. The present section is devoted to an analysis of this phenomenon.

As we saw in the preceding section, the power spectrum, $\langle\tilde{\mathbf{E}}_s^{(-)}(\hat{\mathbf{r}},\tilde{\omega})\cdot\tilde{\mathbf{E}}_s^{(+)}(\hat{\mathbf{r}},\tilde{\omega})\rangle$, of scattered light has a Lorenzian frequency dependence,

$$B(\omega)=\frac{1}{\gamma^2+(\omega_0-\omega)^2},$$

which gives it a characteristic width γ. In our calculation, we have assumed that γ is a constant, independent of the external state of the atom. Now we want to calculate this quantity more carefully to see if that is indeed so.

As before, we assume the atom has only two electronic states, the ground state $|G\rangle$ and the excited state $|E\rangle$, and lives in a three-dimensional potential well described accurately in the parabolic approximation. The Hamiltonian for the atom interacting with the electromagnetic field has the form

$$H=\hbar\omega_0|E\rangle\langle E|+P^2/(2m)+\chi R^2/2+V_I+\sum_{\mathbf{k}_v}\hbar\omega_{\mathbf{k}_v}a^\dagger_{\mathbf{k}_v}a_{\mathbf{k}_v}, \tag{35}$$

where the operators $\{a^\dagger_{\mathbf{k}_v}\}$ and $\{a_{\mathbf{k}_v}\}$ are the photon creation and annihilation operators. The interaction between the atom and the vacuum field $\mathbf{E}_{vac}$, described by the term V_I, causes a spontaneous relaxation of the atom from an excited state to a lower state by the emission of a photon.

Let us assume that initially the atom is in the internal excited state $|E\rangle$ and in the external motional state $|l\rangle$, while the field is in the vacuum state $|0\rangle$. Because of its interaction with the electromagnetic field, the atom tends to relax into the internal ground state $|G\rangle$ and possibly another external state $|n\rangle$, emitting a photon of wave vector $\mathbf{k}_v$ and polarization $\mathbf{e}$ in the state $|\mathbf{k}_v\mathbf{e}\rangle$. We find it convenient to use the Weisskopf-Wigner method [40] to construct an intermediate state $|\psi(t)\rangle$ as the following superposition of the initial state and all possible final states:

$$|\psi(t)\rangle=b_1(t)|E,l,0\rangle e^{-i(E_1t/\hbar)}+\sum_{\mathbf{K}_v\mathbf{e}}b_2^{\mathbf{k}_v\mathbf{e}}(t)|G,n,\mathbf{k}_v\mathbf{e}\rangle e^{-i(E_2t/\hbar)}, \tag{36}$$

with the caveats $b_1(t)=e^{-\gamma t}$ and $b_2^{\mathbf{k}_v\mathbf{e}}(0)=0$. The parameter γ is the decay constant, and $E_1=E+(l+1/2)\hbar\overline{\omega}$ and $E_2=G+(n+1/2)\hbar\overline{\omega}+\hbar\omega_{\mathbf{k}_v}$ are the energy eigenvalues of the two states $|E,l,0\rangle$ and $|G,n,\mathbf{k}_v\mathbf{e}\rangle$. By substituting Eq. (36) into the Schrödinger equation generated by the Hamiltonian (35) and then performing appropriate scalar products, we obtain the following differential equations for $b_1(t)$ and $b_2^{\mathbf{k}_v\mathbf{e}}(t)$:

$$i\hbar\dot{b}_1(t)=\sum_{\mathbf{k}_v\mathbf{e}}b_2^{\mathbf{k}_v\mathbf{e}}(t)\langle E,N,0|V_I|G,n,\mathbf{k}_v\mathbf{e}\rangle e^{i\omega_{12}t}, \tag{37}$$

$$i\hbar\dot{b}_2^{\mathbf{k}_v\mathbf{e}}(t)=b_1(t)\langle G,n,\mathbf{k}_v\mathbf{e}|V_I|E,N,0\rangle e^{-i\omega_{12}t}, \tag{38}$$

where $\omega_{12}=\omega_0+(l-n)\overline{\omega}-\omega_{\mathbf{k}_v}$.

Equation (38) may be integrated in time when the form $b_1(t)=e^{-\gamma t}$ is substituted into it and the initial condition, $b_2^{\mathbf{k}_v\mathbf{e}}(0)=0$ is used, with the result

$$b_2^{\mathbf{k}_v\mathbf{e}}(t)=\frac{i}{\hbar}\langle G,n,\mathbf{k}_v\mathbf{e}|V_I|E,l,0\rangle\frac{-1+e^{-i\omega_{12}t-\gamma t}}{\gamma+i\omega_{12}}. \tag{39}$$

We can now calculate γ by substituting this expression for $b_2^{\mathbf{k}_v\mathbf{e}}$ into Eq. (37),

$$-i\hbar\gamma=\sum_{\mathbf{k}_v\mathbf{e}}\frac{i}{\hbar}|\langle G,n,\mathbf{k}_v\mathbf{e}|V_I|E,l,0\rangle|^2\frac{1-e^{i\omega_{12}t+\gamma t}}{\gamma+i\omega_{12}}. \tag{40}$$

Using the approximation of Ref. [41] to replace $(1-e^{i\omega_{12}t+\gamma t})/(\gamma+i\omega_{12})$ by the sum of a δ function and a Cauchy principal value form, we can thus calculate γ. Its real part gives the transition rate from an excited state to a lower state, and its imaginary part the radiative level shift. Both the radiative decay and level shift are characteristic of a discrete state coupled to a continuum. Since the transition rate is all we care for, however, we need to retain only the real part of γ [42]. By replacing the sum over $\mathbf{k}_v$ by an integral, valid in the limit of infinite quantization volume L^3 [37], we obtain the result

$$\gamma\simeq\frac{\pi}{\hbar^2}\int d\mathbf{k}_v\sum_{\mathbf{e}}\left(\frac{L}{2\pi}\right)^3|\langle G,n,\mathbf{k}_v\mathbf{e}|V_I|E,l,0\rangle|^2\times\delta(\omega_{\mathbf{k}_v}-\omega_0-(l-n)\overline{\omega}). \tag{41}$$

The matrix element of V_I present in Eq. (41) reduces in the rotating-wave approximation to the form

$$\langle G,n,\mathbf{k}_v\mathbf{e}|V_I|E,l,0\rangle=\langle G,n,\mathbf{k}_v\mathbf{e}|-i\mathbf{d}_{op}\cdot\sum_j\nu_j a_j\hat{\boldsymbol{\epsilon}}e^{i\mathbf{k}_j\cdot\mathbf{r}}+i\mathbf{d}^\dagger_{op}\cdot\sum_j\nu_j a^\dagger_j\hat{\boldsymbol{\epsilon}}e^{-i\mathbf{k}_j\cdot\mathbf{r}}|E,l,0\rangle, \tag{42}$$

where $(\mathbf{d}_{op}+\mathbf{d}^\dagger_{op})$ is the atomic dipole operator, $\nu_j=\sqrt{2\pi\hbar\omega_j/L^3}$, and j is an abbreviated notation to label a particular wave-vector-polarization mode of light. Only $a^\dagger_j$ contributes to the preceding matrix element. Assuming that $\mathbf{d}_{op}$ is along $\hat{z}$, we then have

$$\langle G,n,\mathbf{k}_v\mathbf{e}|V_I|E,l,0\rangle = id(\hat{z}\cdot\hat{\boldsymbol{\epsilon}}_{\mathbf{k}_v\mathbf{e}})\nu_{k_v}\langle n|e^{-i\mathbf{k}_v\cdot\mathbf{r}}|l\rangle. \quad (43)$$

Substituting Eq. (43) back into Eq. (41), and splitting the $\mathbf{k}_v$ integration into its radial and angular parts, we obtain

$$\gamma = \frac{d^2}{\hbar 4\pi}\sum_{\mathbf{e}}\int d\omega_{\mathbf{k}_v\mathbf{e}}\frac{\omega_{\mathbf{k}_v}^3}{c^3}\int d\Omega(\hat{z}\cdot\hat{\boldsymbol{\epsilon}}_{\mathbf{k}_v\mathbf{e}})^2|\langle n|e^{-i\mathbf{k}_v\cdot\mathbf{r}}|l\rangle|^2 \times\delta(\omega_{\mathbf{k}_v}-\omega_0-(l-n)\bar{\omega}), \quad (44)$$

where $d\Omega$ is the solid angle element associated with the direction of $\mathbf{k}_v$. This is the general formula for the decay rate.

Let us assume that initially the atom is in the ground motional state, $l=0$, for which the matrix element $\langle n|e^{-i\mathbf{k}_v\cdot\mathbf{r}}|0\rangle$ can be evaluated by noting that

$$i\mathbf{k}_v\cdot\mathbf{r} = i\sqrt{\frac{\hbar}{2m\bar{\omega}}}(k_{vx})(a_x+a_x^\dagger)+i\sqrt{\frac{\hbar}{2m\bar{\omega}}}(k_{vy})(a_y+a_y^\dagger) + i\sqrt{\frac{\hbar}{2m\bar{\omega}}}(k_{vz})(a_z+a_z^\dagger). \quad (45)$$

In other words, $e^{i\mathbf{k}_v\cdot\mathbf{r}}$ is a three-dimensional displacement operator [37], which produces a three-dimensional coherent state when operated on the motional ground state. This observation enables us to write down

$$\langle n|e^{-i\mathbf{k}_v\cdot\mathbf{r}}|0\rangle = e^{-\hbar k_v^2/4m\bar{\omega}}\frac{1}{\sqrt{n_x!n_y!n_z!}}\left(-ik_{vx}\sqrt{\frac{\hbar}{2m\bar{\omega}}}\right)^{n_x} \times\left(-ik_{vy}\sqrt{\frac{\hbar}{2m\bar{\omega}}}\right)^{n_y}\left(-ik_{vz}\sqrt{\frac{\hbar}{2m\bar{\omega}}}\right)^{n_z}. \quad (46)$$

With this result, we can go on to express γ as

$$\gamma = \frac{d^2}{\hbar 4\pi}\sum_{\mathbf{e}}\int k^3 d\Omega e^{-\hbar k^2/2m\bar{\omega}}\frac{1}{n_x!n_y!n_z!} \times(k_x)^{2n_x}(k_y)^{2n_y}(k_z)^{2n_z}(\hbar/2m\bar{\omega})^{n_x+n_y+n_z}(\hat{z}\cdot\hat{\boldsymbol{\epsilon}}_{\mathbf{k}_v\mathbf{e}})^2, \quad (47)$$

where we have set $k=k_v=(\omega_0-n\bar{\omega})/c$. Introducing θ and ϕ, the polar and azimuthal angles of $\mathbf{k}$ relative to $\hat{z}$, we can perform the sum $\Sigma_{\mathbf{e}}(\hat{z}\cdot\hat{\boldsymbol{\epsilon}}_{\mathbf{k}_v\mathbf{e}})^2$ [28] and show it to equal $\sin^2\theta$. This result when substituted into Eq. (47) leads to a simple angular integral that can be evaluated in closed form,

$$\gamma = \gamma_0\frac{3}{8\pi}e^{-(\hbar k^2/2m\bar{\omega})}\frac{1}{n_x!n_y!n_z!}(\hbar k^2/2m\bar{\omega})^{n_x+n_y+n_z}I_\theta I_\phi, \quad (48)$$

where $\gamma_0=(2d^2k^3/3\hbar)$ is the Wigner-Weisskopf natural decay rate for an isolated atom at rest and I_θ, I_ϕ involve certain Γ functions

$$I_\theta = \frac{\Gamma(n_z+1/2)\Gamma(n_x+n_y+2)}{\Gamma(n_x+n_y+n_z+5/2)}, \quad (49)$$

$$I_\phi = 2\frac{\Gamma(n_y+1/2)\Gamma(n_x+1/2)}{\Gamma(n_x+n_y+1)}. \quad (50)$$

In an isotropic harmonic potential well, all excited states with the same value for the sum of $(n_x+n_y+n_z)$ are degenerate. Therefore, the transition rate corresponding to a radiated photon with a wave number $k=(\omega-n\bar{\omega})/c$ is the sum of transition rates into individual components in the subset of n_x,n_y,n_z values that add up to n:

$$\Gamma_{trans}^n = \gamma_0\frac{3}{8\pi}e^{-(\hbar k^2/2m\bar{\omega})}\sum_{n_x+n_y+n_z=n} \times\left[\frac{1}{n_x!n_y!n_z!}\left(\frac{k^2\hbar}{2m\bar{\omega}}\right)^{n_x+n_y+n_z}I_\theta I_\phi\right]. \quad (51)$$

For a typical experimental situation, $\Gamma_{trans}^n<\gamma_0$, i.e., the widths of the sidebands are narrower than expected, a fact verified by experiments [33]. From Eq. (51), we can see that the Lamb-Dicke effect is the principal contribution to this narrowing. Although the degeneracy of the external atomic states tends to oppose the line narrowing, it is overwhelmed by the Lamb-Dicke contribution. The physical origin of this narrowing is the small overlap between an excited state and the ground state of harmonic motion.

When the optical potential well is so stiff that $\bar{\omega}\to\infty$, then only $n_x=n_y=n_z=0$ will contribute to the sum in Eq. (51). We then have

$$\Gamma_{trans}^n = \gamma_0. \quad (52)$$

Physically speaking, in this case the atom is tightly trapped in the ground state of the harmonic motion and therefore radiates like a stationary radiator.

VI. CONCLUSION

In this paper, we have discussed Born scattering from an optical lattice formed by trapped atoms, and found that by studying the scattered intensity, we can obtain important information about the lattice, such as the lattice constant, the stiffness of the individual optical traps, and the number of trapped atoms. We also studied the angular coherence of the scattered light both at the frequency of the incident light and at its motional sidebands. Finally, we explained an observed narrowing of the sideband spectral lines as an essential consequence of the Lamb-Dicke effect.

Born scattering is a powerful tool to monitor the motion of the trapped atoms. It does not, however, give us much insight into how light propagates inside an optical lattice. One must take into account the higher orders of scattering if the nature of light propagation inside a strongly scattering medium is to be fully understood. We turn to this question in paper II [10].

[1] A. Ishimaru, *Wave Propagation and Scattering in Random Media* (Academic, New York, 1978).
[2] A. Lagendijk and M. van Albada, Phys. World **3**(1), 33 (1990).
[3] Y. Kuga and A. Ishimaru, J. Opt. Soc. Am. A **1**, 831 (1984).
[4] M.P. van Albada and A. Lagendijk, Phys. Rev. Lett. **55**, 2692 (1985).
[5] P.E. Wolf and G. Maret, Phys. Rev. Lett. **55**, 2696 (1985).
[6] L. Tsang and A. Ishimaru, J. Opt. Soc. Am. A **2**, 1331 (1985).
[7] M.B. van der Mark, M.P. van Albada, and A. Lagendijk, Phys. Rev. B **37**, 3575 (1988).
[8] Diederik S. Wiersma, Paolo Bartolini, Ad Lagendijk, and Roberto Righini, Nature (London) **390**, 671 (1997).
[9] D.J. Wineland and W.M. Itano, Phys. Today **40**(6), 34 (1987).
[10] Wei Guo and Sudhakar Prasad, following paper, Phys. Rev. E **67**, 056615 (2003).
[11] H.C. van de Hulst, *Multiple Light Scattering* (Academic, New York, 1980).
[12] K.J. Peters, Phys. Rev. B **46**, 801 (1992).
[13] C.E. Mandt, L. Tsang, and A. Ishimaru, J. Opt. Soc. Am. A **7**, 585 (1990).
[14] F.C. MacKintosh and S. John, Phys. Rev. B **37**, 1884 (1988).
[15] B.A. van Tiggelen, Phys. Rev. Lett. **75**, 422 (1995).
[16] G.L.J.A. Rikken and B.A. van Tiggelen, Nature (London) **381**, 54 (1996).
[17] F.A. Erbacher, R. Lenke, and G. Maret, Europhys. Lett. **21**, 551 (1993).
[18] A.S. Martinez and R. Maynard, Phys. Rev. B **50**, 3714 (1994).
[19] A. Hemmerich and T.W. Hänsch, Phys. Rev. Lett. **70**, 410 (1993).
[20] G. Grynberg, B. Lounis, P. Verkerk, J.-Y. Courtois, and C. Salomon, Phys. Rev. Lett. **70**, 2249 (1993).
[21] K.I. Petsas, A.B. Coates, and G. Grynberg, Phys. Rev. A **50**, 5173 (1994).
[22] P.S. Jessen and I.H. Deutsch, Adv. At., Mol., Opt. Phys. **37**, 95 (1996).
[23] J.-Y. Courtois and G. Grynberg, Phys. Rev. A **46**, 7060 (1992).
[24] We assume that there is no mutual atomic interaction [26] between neighboring atoms.
[25] Typically $\gamma \sim 10^8 (1/s)$, while $\bar{\omega} \sim 10^4 (1/s)$.
[26] M.M. Burns, J.-M. Fournier, and J.A. Golovchenko, Science (Washington, DC, U.S.) **249**, 749 (1990).
[27] Chen-To Tai, *Dyadic Green's Functions in Electromagnetic Theory*, 1st ed. (Intext Educational, Scranton, 1971).
[28] Claude Cohen-Tannoudji, Jacques Dupont-Roc, and Gilbert Grynberg, *Atom-Photon Interaction: Basic Processes and Applications*, 1st ed. (Wiley-Interscience, New York, 1992).
[29] N.W. Ashcroft and N.D. Mermin, *Solid State Physics* (Holt, Rinehart and Winston, New York, 1976).
[30] Such a low occupation rate, however, will not prohibit the observation of Bragg scattering [31]. The reason is as long as $\mathbf{k}_1$ satisfies the Bragg scattering condition [29], all the wavelets from the lattice sites will be in phase.
[31] M. Weidemüller, A. Hemmerich, A. Görlitz, T. Esslinger, and T.W. Hänsch, Phys. Rev. Lett. **75**, 4583 (1995).
[32] M. Gatzke, G. Birkl, P.S. Jessen, A. Kastberg, S.L. Rolston, and W.D. Phillips, Phys. Rev. A **55**, R3987 (1997).
[33] C.I. Westbrook, C. Jurczak, G. Birkl, B. Desruelle, W.D. Phillips, and A. Aspect, J. Mod. Opt. **44**, 1837 (1997).
[34] R.H. Dicke, Phys. Rev. **89**, 473 (1953).
[35] The sideband generation has its origin in the periodic motion of the radiator. It can also be discussed classically [34].
[36] M. Weidemüller, A. Görlitz, T.W. Hänsch, and A. Hemmerich, Phys. Rev. A **58**, 4647 (1998).
[37] L. Mandel and E. Wolf, *Optical Coherence and Quantum Optics* (Cambridge University Press, New York, 1995).
[38] We choose for definiteness N_x, N_y, and N_z to be even numbers.
[39] J.W. Goodman, *Statistical Optics* (Wiley, New York, 1985).
[40] W. Heitler, *The Quantum Theory of Radiation*, 3rd ed. (Clarendon, Oxford, 1954).
[41] H. Haken, *Light* (North-Holland, New York, 1981), Vol. 1.
[42] Equation (41) can also be derived directly [28] by using Fermi's golden rule. The advantage of the present approach adopted here is that it also gives an expression for the energy shift simultaneously.